INEEL/CON-2000-00579
PREPRINT

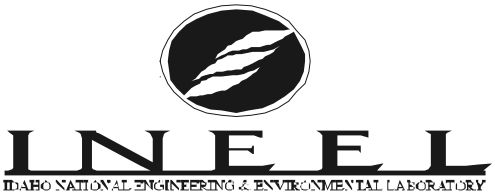

Ultrasonic Imaging and Theoretical Prediction of Orthotropic Plate Stiffness in all Planar Directions

K. L. Telschow (INEEL)
V. A. Deason (INEEL)
O. Mukdadi (U of Colorado)
S. K. Datta (U of Colorado)

July 16, 2000 – July 21, 2000

27th Annual Review of Progress in Quantitative NDE

BECHTEL BWXT IDAHO, LLC

ULTRASONIC IMAGING AND PREDICTION OF ORTHOTROPIC PLATE STIFFNESS IN ALL PLANAR DIRECTIONS

Subhendu K. Datta[1], Osama Mukdadi[1], Kenneth L. Telschow[2], and Vance A. Deason[2]

[1]Dept. of Mechanical Engineering, University of Colorado, Boulder, CO 80309-0427

[2]Idaho National Engineering and Environmental Laboratory, Idaho Falls, ID 83415-2209

Abstract. Exact and approximate theoretical analysis of the wavelengths of plate wave mode propagation in all planar directions for the dispersive antisymmetric Lamb wave mode are compared with measurements from a laser ultrasonic imaging approach that records the out of plane ultrasonic motion over a large area in a single frame without scanning. Good agreement is demonstrated, based on independent determination of the elastic constants, for two different types of paper.

INTRODUCTION

In the paper industry, accurate measurement and control of paper stiffness is desired. Ultrasonic methods offer a means of determining stiffness, since elastic wave speeds depend on the local stiffness or elastic constants. Studies have shown a strong correlation between the quality (strength, fiber orientation, and other mechanical properties) of paper and its elastic constants. Traditionally, contact ultrasonic methods have been employed to measure the elastic constants [1,2]. Piezoelectric transducers are placed in contact with the paper surface to generate and detect plate wave modes in the paper [3]. At low frequencies, there are three propagating modes: anti-symmetric or flexural, A_0, the anti-plane symmetric or shear horizontal, SH_0, and the symmetric or extensional, S_0. In paper, the phase velocities of the first and third of these modes are readily measured and results of propagation of these modes in the machine direction (MD) and the cross direction (CD) provide important parameters depicting the higher stiffness in the paper along the MD direction.

A new approach for elastic wave measurements that does not require the transducers to be in physical contact with the paper is provided by laser ultrasonics; a technique that employs lasers to both generate and detect elastic wave motion at the surface of materials. A pulsed laser delivers a high intensity but very short impulse to the paper through absorption of light at the surface. Both thermoelastic expansion, at low energies, or ablation of material, at high energies, generate elastic waves in paper. Operation in the thermoelastic regime is non-damaging and well understood but usually much less efficient than the ablation regime. Typically, an optical interferometer serves for detection by demodulating the small phase modulation that the elastic wave motion produces on a

Submitted to the 27th Annual Review of Progress in Quantitative Nondestructive Evaluation, Ames, Iowa July 16-21, 2000

continuous probe laser beam. The laser ultrasonic technique has been used to measure elastic properties of thin plates and paper [4,5]. Laser ultrasonics offers great potential for implementation in the field and even in situ during the paper making process [6,7]. In order to fully utilize this approach for industrial monitoring and control of paper manufacturing, it is necessary to have accurate and reliable measurements that agree well with theoretical modeling of the elastic anisotropic properties that relate to paper microstructure. Currently, in situ measurements are being pursued by scanning single point measurements over the paper surface coupled with theoretical modeling of paper anisotropy restricted to principal directions. However, more information about the paper microstructure (such as texture orientation with respect to the drawing direction) is available from ultrasonic measurements through (1) accounting for orthotropic anisotropy in all planar directions of the paper (i.e. along directions other than the elastic symmetry axes), (2) utilization of additional properties of anisotropic plate wave modes, and (3) implementation of full field imaging of elastic wave propagation. Theoretical and experimental approaches are presented here that begin to fulfill these requirements.

As mentioned above, there are three principal modes of guided waves in plates. These principal modes and their speeds are dependent upon material anisotropy, thickness, and density of the paper (considered here as an elastic plate). For example, a propagating wave along a symmetry axis of an orthotropic plate can be classified as a symmetric longitudinal wave, an anti-symmetric flexural wave or a symmetric or anti-symmetric SH wave. Here, symmetry and anti-symmetry are defined with respect to the mid-plane of the plate. In general, however, for propagation along other directions, the SH mode is coupled with the other modes. Thus, the displacement has all three components. In this paper, prediction of propagation properties along all planar directions as well as this coupling is analyzed in detail. Specific results for the lowest anti-symmetric mode propagation in all planar directions are presented. In addition, it is demonstrated that strong coupling occurs at certain frequencies where a predominantly SH mode changes to a different mode.

Early modeling and experimental work on paper, as an orthotropic thin plate, was addressed by Habeger, et.al., [8]. Cheng and Berthelot [5] examined the sensitivity of the wave speeds to deviations in the elastic constants from the average. Their work on paper was limited to propagation along principal axes. In this study, we present the results of an exact solution for Lamb waves in a thin orthotropic plate using a matrix method analogous to that used by Niklasson, et.al., [9] for guided waves in a metallic plate with thin anisotropic superconducting surface layers and by Mal [10] for composite plates. Furthermore, a first order approximate thin plate theory following Mindlin [11,12] is also presented to obtain approximate solutions for anti-symmetric (flexural) wave motion along an arbitrary planar direction in a thin orthotropic plate. Numerical results are presented showing the dispersion and coupling of the modes of propagation in actual paper samples.

Recently, a full-field laser ultrasonic imaging approach has been developed that provides a complete measurement of the elastic waves in paper traveling in all planar directions simultaneously, *without scanning* single point measurement devices [13,14]. This full-field imaging technique offers great potential for increasing the speed of measurement and ultimately provides more information as to local property variations and flaws in the paper. Image data are optically (as opposed to computationally) processed so as to present a video image of the paper with the ultrasonic wavefronts superimposed on the image. The shape and distribution of the acoustic wavefronts provide information about the wave speed and material properties in all directions within the plane of the paper simultaneously, displaying in a single image such properties as anisotropy, orientation and local inhomogeneities. The method uses continuous or tone burst excitation and heterodyne

interference to produce a near real-time picture of the elastic wavefront propagation. In addition, simple processing of the image with the Fourier transform provides an image of wave slowness (or reciprocal wavelength) and elastic anisotropy in all planar directions from a single image. Good agreement is presented between the theoretical modeling results and the experimental measurements.

THEORETICAL PREDICTION

Paper microstructure is usually modeled by orthotropic elastic anisotropy with nine elastic constants, the symmetry axes are aligned along the fibers, i.e. along MD, CD, and the thickness direction (ZD). These axes are chosen to coincide respectively with the rectangular coordinate axes (x, y, z) in this work. Let u, v, and w be the dynamic displacement components along x, y, and z axes, respectively. The constitutive equation for paper may be written as,

$$\begin{Bmatrix} \sigma_{xx} \\ \sigma_{yy} \\ \sigma_{zz} \\ \sigma_{yz} \\ \sigma_{xz} \\ \sigma_{xy} \end{Bmatrix} = \begin{bmatrix} C_{11} & C_{12} & C_{13} & . & . & . \\ & C_{22} & C_{23} & . & . & . \\ & & C_{33} & . & . & . \\ & & & C_{44} & . & . \\ & & & & C_{55} & . \\ symm. & & & & & C_{66} \end{bmatrix} \begin{Bmatrix} \varepsilon_{xx} \\ \varepsilon_{yy} \\ \varepsilon_{zz} \\ \gamma_{yz} \\ \gamma_{zx} \\ \gamma_{xy} \end{Bmatrix} \tag{1}$$

where ε_{IJ} is the linear axial strain, and γ_{IJ} is the engineering shear strain. For small displacements, the equation of motion is given by

$$\sigma_{ji,j} + f_i = \rho \frac{\partial^2 u_i}{\partial t^2}. \tag{2}$$

Anti-Symmetric (Flexural) Motion – Thin Plate Approximation:

The displacement components for anti-symmetric wave motion are expressed as,

$$\tilde{u}(x, y, z, t) = z\psi(x, y, t), \quad \tilde{v}(x, y, z, t) = z\phi(x, y, t), \quad \tilde{w}(x, y, z, t) = w(x, y, t) \tag{3}$$

where w is the infinitesimal displacement component along the z axis, and (ϕ, ψ) are the rotations of the normal of the mid-plane about x and y axes components, respectively. The corresponding strain components become

$$\begin{aligned} &\varepsilon_{xx} = z\psi_x(x, y, t), \quad \varepsilon_{yy} = z\phi_y(x, y, t), \quad \varepsilon_{zz} = -\left(C_{13}\varepsilon_{xx} + C_{23}\varepsilon_{yy}\right)/C_{33} \\ &\gamma_{yz} = k_1\left(\phi(x, y, t) + w_y(x, y, t)\right), \quad \gamma_{zx} = k_2\left(\psi(x, y, t) + w_x(x, y, t)\right) \\ &\gamma_{xy} = z\left(\psi_y(x, y, t) + \phi_x(x, y, t)\right) \end{aligned} \tag{4}$$

where (k_1, k_2) are correction factors introduced in order to account for errors made in the prediction of the exact cut-off frequencies due to the approximation. Integrating the z-component of the equation of motion and z - times the x & y components with respect to z from $-h$ to $+h$, we obtain the following plate equations of motion,

$$\frac{\partial Q_x}{\partial x}+\frac{\partial Q_y}{\partial y}=2\rho h w_{tt},\ \frac{\partial M_x}{\partial x}+\frac{\partial M_{xy}}{\partial y}-Q_x=\frac{2}{3}\rho h^3\psi_{tt},\ \frac{\partial M_{xy}}{\partial x}+\frac{\partial M_y}{\partial y}-Q_y=\frac{2}{3}\rho h^3\phi_{tt} \qquad (5)$$

where the stress and moment resultants are

$$(Q_x, Q_y)=\int_{-h}^{h}(\sigma_{zx},\sigma_{yz})dz,\quad (M_x, M_{xy}, M_y)=\int_{-h}^{h}z(\sigma_{xx},\sigma_{xy},\sigma_{yy})dz \qquad (6)$$

Taking the Fourier transform, we obtain a linear eigenvalue problem as,

$$\left(\begin{bmatrix} k_2^2k_x^2C_{55}+k_1^2k_y^2C_{44} & -ik_2^2k_xC_{55} & -ik_1^2k_yC_{44} \\ ik_2^2k_xC_{55} & k_2^2C_{55}+\frac{h^2}{3}\left(k_x^2\overline{C}_{11}+k_y^2C_{66}\right) & \frac{h^2}{3}k_xk_y\left(\overline{C}_{12}+C_{66}\right) \\ ik_1^2k_yC_{44} & \frac{h^2}{3}k_xk_y\left(\overline{C}_{12}+C_{66}\right) & k_1^2C_{44}+\frac{h^2}{3}\left(k_y^2\overline{C}_{22}+k_x^2C_{66}\right) \end{bmatrix} - \omega^2\begin{bmatrix} \rho & . & . \\ . & \frac{\rho h^2}{3} & . \\ . & . & \frac{\rho h^2}{3} \end{bmatrix}\right)\begin{Bmatrix}\hat{w}\\ \hat{\psi}\\ \hat{\phi}\end{Bmatrix}=\begin{Bmatrix}0\\0\\0\end{Bmatrix} \qquad (7)$$

where $\overline{C}_{11}=C_{11}-C_{13}^2/C_{33}$, $\overline{C}_{12}=C_{12}-C_{13}C_{23}/C_{33}$, and $\overline{C}_{22}=C_{22}-C_{23}^2/C_{33}$. Solving the eigenvalue problem leads to the dispersion relation for the modes A_0, A_1, and SH_1. The correction factors k_1 and k_2 can be determined by equating the cut-off frequencies for the SH_1 and A_1 modes, respectively, given by the approximate and exact solutions with $k_1^2=\frac{h^2\omega^2}{3C_{44}/\rho}=\frac{1}{3}\left(\frac{\pi}{2}\right)^2$ and $k_2^2=\frac{h^2\omega^2}{3C_{55}/\rho}=\frac{1}{3}\left(\frac{\pi}{2}\right)^2$.

Theoretical Numerical Predictions

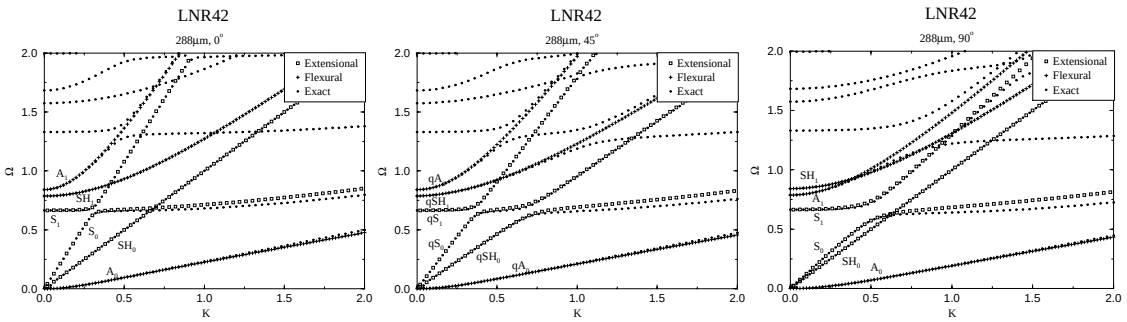

(a) (b) (c)

FIGURE 1. Exact and approximate dispersion curves for wave propagation along (a) MD-axis, (b) 45^o off MD-axis, (c) CD-axis for LNR42 paper.

The exact dispersion equation was solved for two types of paper, raw stock (copy) - RSK59 and linerboard - LNR42, that were experimentally measured using the laser ultrasonic imaging technique. The elastic constants for these papers were independently measured by contact piezoelectric ultrasonic methods at the Institute of Paper Science and Technology [15] and are presented in Table 1.

Dispersion curves were calculated for different planar wave propagation angles measured from the MD. Predictions of the thin plate theory approximation for the extensional and flexural modes with the exact and approximate solutions are compared in Figure 1 for propagation along MD, 45^o, and CD directions. In these figures $\Omega = 2\omega h \Big/ \sqrt{C_{66}/\rho}$ and $\mathrm{K} = 2kh$, where $k_x = \mathrm{K}\cos\alpha$ and $k_y = \mathrm{K}\sin\alpha$, α being the angle made by the propagation direction with the x-axis. It is seen that for propagation along the MD (Figure 1a), the thin plate theory predicts the dispersion curve of the first two extensional modes quite well up to $\mathrm{K} \cong 0.75$. For the A_0 mode, the agreement holds for larger values of K. The mode interchange shown for off-symmetry axes propagation (Figure 1b), for the extensional and shear-horizontal modes, is predicted well by the thin plate theory and can be used to determine the in-plane elastic constants C_{66} and C_{12}.

EXPERIMENTAL DYNAMIC HOLOGRAPHIC IMAGING

A new approach to imaging ultrasonic wave motion is under investigation at the Idaho National Engineering and Environmental Laboratory (INEEL). This approach utilizes nonlinear optical photorefractive methods to perform interferometric detection over an extended area within a single image frame. Without scanning, this method provides a complete and continuous image of the out of plane elastic wave motion in paper as the wave simultaneously travels in all directions within the plane of the paper sheet. This approach is based on optical dynamic holographic methods that record the phase distribution over large areas of the paper surface simultaneously. Previous use of conventional holographic techniques have demonstrated the ability of this approach to image flexural waves in paper [16]. Full-field imaging offers excellent potential for

TABLE 1. Elastic constants C_{ij} (GPa), density ρ (Kg/m^3), and thickness $2h$ (μm) of the paper samples.

Paper	C_{11}	C_{22}	C_{33}	C_{44}	C_{55}	C_{66}	C_{12}	C_{13}	C_{23}	ρ	$2h$
RSK59	9.85	4.95	0.14	0.20	0.21	2.53	1.77	0.10	0.15	818	110
LNR42	10.3	3.70	0.10	0.14	0.16	2.23	1.82	0.10	0.15	742	288

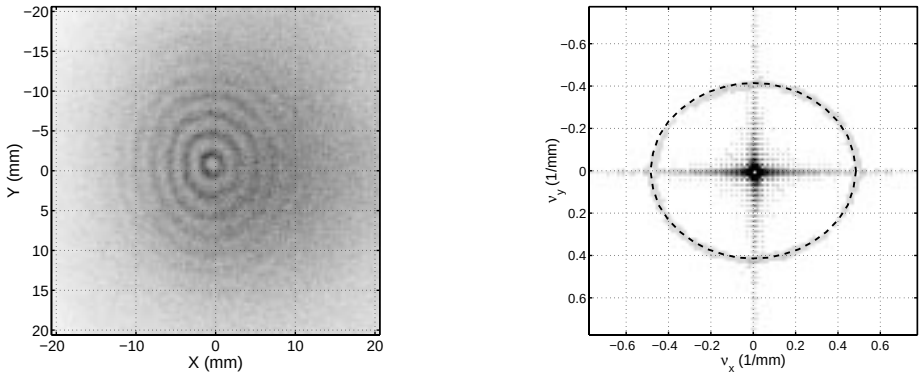

(a) (b)

Figure 2. (a) Image of the A_0 mode wavefront recorded at 100 kHz in a 110 μm thick sheet of RSK59 paper, (b) Image of the FFT magnitude of the A_0 mode wavefront as a function of reciprocal wavelength ($\nu=1/\lambda$). The dashed line is the independent prediction based on IPST paper parameters from Eq. (7) for this operating frequency.

increasing the speed of the measurement and it ultimately will provide more information of local property variations and flaws in the paper. However, until recently, this was a very difficult measurement as it required holographic methods that were intrinsically laboratory based. The photorefractive approach employed here provides an adaptive dynamic alternative to the older static holographic methods. The capabilities of the method to yield information from measurement of dispersive flexural waves are presented that agree well with the theoretical predictions for propagation in all planar directions. The basic operation of the imaging ultrasonic camera system has been previously described [17,18,19].

Ultrasonic waves were generated from continuous wave (CW) point contact piezoelectric excitation at frequencies from 10 kHz to 1 MHz on the reverse side of the sheets of paper. The paper was illuminated with a laser beam that had been expanded to cover the area of interest. Images captured sequentially at a nonzero camera frame rate show wavefronts emanating from a central excitation point traveling outward. Continuous viewing of the sequence provides a pseudo real-time image of propagating ultrasonic wavefronts. The A_0 mode under CW excitation was utilized for this study. The relatively low speed of this mode and its frequency dispersion allowed for considerable adjustment of the ultrasonic wavelengths observed. The effects of dispersion were easily taken into account by precise determination of the wavelength as a function of frequency. The paper samples were vertically supported in an 18 cm diameter aluminum ring. Figures 2a & 3a show images taken with the INEEL camera of the ultrasonic wavefronts at 100 kHz, on RSK59 and LNR42 paper, respectively. Note that the ultrasonic wavefronts are clearly shown in all directions at once over 20 x 20 mm and 30 x 30 mm regions. Each is an image obtained by averaging in phase and out of phase frames to suppress the background surface image. The anisotropic nature of the ultrasonic wave propagation is clearly visible in all the images as well as laser speckle.

Figures 2b & 3b show the corresponding magnitudes of the two dimensional Fourier transforms of the spatial images. Fourier transform of the displacement image results in an image of the "slowness" diagram for this material; that is, an image showing the wavenumber ($1/\lambda_a$) in all directions, where λ_a is the ultrasonic A_0 mode wavelength at the measurement frequency. Processing the spatial image in this manner is particularly convenient, as it utilizes all the data the image provides. Even measurements with much reduced signal to noise ratio, as seen for the LNR42 image, still result in useable images for comparison to the theoretical predictions. Superimposed onto the Fourier transform images for the two paper samples are the resulting predictions from the approximate thin plate theory described earlier. There are no adjustable parameters in this comparison. The theoretical predictions are based entirely on the elastic coefficients, density, and thickness parameters obtained from the independent IPST measurements. The exceptional agreement between the theoretical predictions and the experimental data from the camera measurements is readily apparent and testifies to the overall accuracy of the entire theoretical and experimental process followed.

A significant advantage of the ultrasonic wave full-field measurement method is the fact that data in all planar propagation directions are obtained simultaneously in one image. This allows one to determine the elastic stiffness in both the MD and CD directions as well as obtain a measure of the alignment of the paper axes with the manufacturing direction. A misalignment produces a rotation of the image. This information would be difficult to obtain from single point measurements, unless a large scanned set of measurements were performed. Detailed analysis of the orientation misalignment is underway.

ACKNOWLEGEMENTS

The authors wish to thank P. Brodeur, C. Habeger, J. Gerhardstein, B. Prufahl, and E. Lafond at the Institute for Paper Science and Technology for characterized paper samples, and for many informative and stimulating discussions of paper physics and paper manufacturing processes. We would also like to thank Scott Watson for his technical efforts related to fabrication and operation of the camera system and for obtaining this data. This work was sponsored by the U.S. Department of Energy, Office of Science, Basic Energy Sciences, Engineering Research Program, and the INEEL Laboratory Directed Research & Development program under DOE Idaho Operations Office Contract DE-AC07-99ID13727. SKD gratefully acknowledges also the support received from the

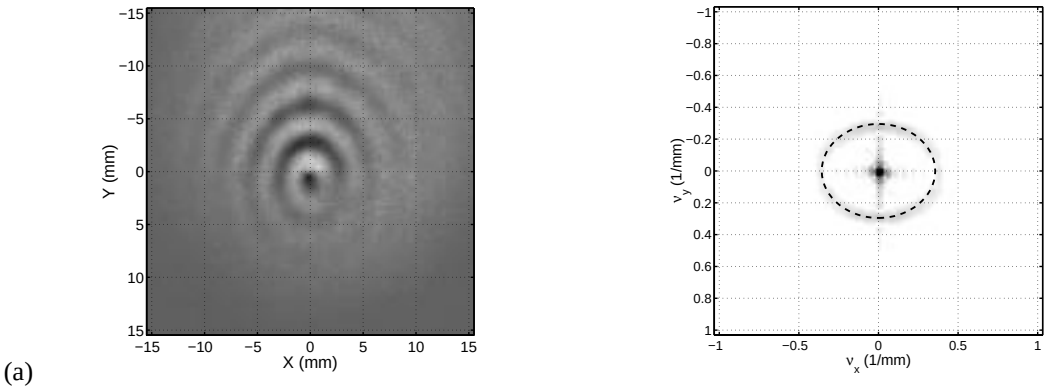

(a)

Figure 3. (a) Image of the A_0 mode wavefront recorded at 100 kHz in a 288 μm thick sheet of LNR42 paper, (b) Image of the FFT magnitude of the A_0 mode wavefront as a function of reciprocal wavelength ($\nu=1/\lambda$). The dashed line is the independent prediction based on IPST paper parameters from Eq. (7) for this operating frequency.

University of Colorado by a Faculty Fellowship award.

REFERENCES

1. Mann, R.W., Baum, G.A., and Habeger, C.C., *Tappi* **63**(2), 163-166 (1980).
2. Habeger, C.C., and Wink, W.A., *J. Appl. Polymer Sci.* **32,** 4503-4540 (1986).
3. Van Zummerman, M., Young, D. , Haberger, C., Baum, G., and Treleven, R., *Ultrasonics* **25,** 288-294 (1987).
4. Johnson, M.A., Berthelot, Y.H. , Brodeur, P.H., and Jacobs, L.A., *Ultrasonics* **34,** 703-710 (1996).
5. Cheng, J.C., and Berthelot, Y.H., *J. Phys. D.* **29,** 1857-1867 (1996).
6. Walter, J.B., Telschow, K.L., Gerhardstein, J.P., Pufahl, B.M., Lafond, E.M., and Brodeur, P.H., "Fabry-Perot Laser Ultrasonic Elastic Anisotropy Measurements in Paper on a Moving Web," in *Reviews of Progress in Quantitative NDE*, **19A** edited by D. O. Thompson and D. E. Chimenti, AIP Conference Proceedings 509, New York, 2000, pp. 247-254.
7. Lafond, E.F., Brodeur, P.H., Gerhardstein, J.P., Habeger, C.C., Jong, J.H., and Telschow, K.L., "Photorefractive Interferometers for Ultrasonic Measurements on Paper," *Ultrasonics*, submitted for publication.
8. Habeger, C.C., Mann, R.W., and Baum, G.A., *Ultrasonics* **17,** 57-62 (1979).
9. Niklasson, A.J., Datta, S.K., and Dunn, M.L., "On approximating guided waves in plates with thin anisotropic coatings by means of effective boundary conditions", *J. Acoust. Soc. Am*., to be published.
10. Mal, A.K., *Wave Motion* **10**, 257-266 (1988).
11. Mindlin, R.D., *J. Appl. Mech.* **18,** 31-38 (1951).
12. Mindlin, R.D., *J. Appl. Phys*. **22,** 316-323 (1951).
13. Deason, V.A., Telschow, K.L., Schley, R.S., Watson, S.M., "Imaging the Anisotropic Elastic Properties of Paper with the *INEEL Laser Ultrasonic Camera*," in *Reviews of Progress in Quantitative NDE*, **19A** edited by D. O. Thompson and D. E. Chimenti, AIP Conference Proceedings 509, New York, 2000, pp. 255-261.
14. Telschow, K.L., and Deason, V.A., "Imaging Anisotropic Elastic Properties of an Orthotropic Paper Sheet Using Photorefractive Dynamic Holography," *Ultrasonics*, submitted for publication.
15. Gerhardtstein, J., Pufahl, B., and Brodeur, P., Institute of Paper Science and Technology, Atlanta, GA, private communication.
16. K. Olofsson and A. Kyosti, "Stiffness and stiffness variation in paper measured by laser generated and laser-recorded bending waves," J. Pulp and Paper Science **20**(11), J328-J333 (1994).
17. Hale, T.C., Telschow, K.L., and Deason, V.A., *Applied Optics*, **111**, 8248–8258 (1997).
18. Telschow, K.L., Deason, V.A., Schley, R.S., and Watson, S.M., "Direct Imaging of Anisotropic Material Properties using Photorefractive Laser Ultrasound," *Nondestructive Characterization Of Materials IX*, edited by R. E. Green, Jr., AIP Conference Proceedings 497, New York, 1999, pp. 162-167.
19. Telschow, K.L., Deason, V.A., Schley, R.S., and Watson, S.M. *J. Acoust. Soc. Am.* **106**(5), 2578-2587 (1999).